Experimental Investigation and Numerical Analysis of the Effect of Temperature on the Mechanical Properties of Aerospace Composite-Metal Hybrid Joints

Rui Hou[1,2], Bintuan Wang[2], Zixun Zhu[1], Weicheng Gao[1]

[1]Department of Astronautical Science and Mechanics, Harbin Institute of Technology (HIT), No. 92 West Dazhi Street, Harbin, 150001, P. R. of China
[2]Department of Strength Design, The First Aircraft Institute of AVIC, Yanliang, Xi'an 710089, P. R. China

Abstract

The study conducted static tensile tests on a triple bolt double-lap joint structure made of CFRP composite and aluminum alloy at three different temperatures (-75℃, 25℃ and 120℃). To predict the failure of composite structures in variable temperature environments, a progressive failure analysis model was employed. The model considers the thermal strain induced by temperature and the influence of temperature on material properties in stress-strain analysis, failure criteria, and damage evolution rules. The model predicts the static strength and failure modes of composite-metal hybrid joints structures at -75°C, 25°C, and 120°C, showing well agreement with experimental results, thereby validating the model's effectiveness. Additionally, it is observed that the mismatch in thermal expansion between composite materials and metals results in the generation of thermal stresses within the structure, altering the location of damage initiation and the failure modes of the structure at low temperatures.

Keywords: Composite-metal hybrid joint; Thermal effects; Strength; Progressive damage model

1. Introduction

Carbon fiber reinforced resin matrix composites (CFRP) have been widely used in the main bearing structures of aerospace vehicles due to their excellent properties such as high strength, high stiffness and light weight [1]. However, due to the complex internal structure of the aircraft and manufacturing process, cost and other conditions, composite materials can not completely replace metal materials [2], so the mixed connection of metal and composite materials is inevitable, and bolt connection because of its stable, reliable, easy to maintain the advantages of the aircraft structure is the most common [3,4]. For the internal connection structure of the aircraft, with the change of service environment temperature, the degradation of mechanical properties of materials and the mismatch of thermal expansion properties will lead to the change of bearing characteristics and failure rules of the hybrid multi-bolt connection structure [5]. Therefore, it is of great significance to study the mechanical properties of metal-composite composite multi-bolt connection at different temperatures. Numerous researchers have conducted experimental research to elucidate the impact of temperature on the structural properties of composite materials. Mariam et al. [6] conducted experimental assessments to investigate the effects of a 50°C humid environment on the tensile failure mechanisms and fatigue failure modes of composite-aluminum alloy bolted joints. Additionally, they examined the progressive decrease in both the stiffness and strength of the bolted joints as the duration of humid-heat aging increased. Turveya et al. [7] conducted experimental research on the load-bearing performance of composite material bolted connections under the influence of temperature environments with varying parameters. They observed that the average failure stress of the structures increased with decreasing temperature but decreased with increasing temperature. Sánchez-Sáez et al. [8] and Vieille et al. [9,10] separately investigated the mechanical behavior of laminated composite plates under extremely low and high temperatures. The results indicate that stiffness increases with decreasing temperature for laminated plates, while high temperatures

enhance the toughness of the matrix resin and degrade the fiber/matrix interface. Abdus et al. [5] investigated the tensile performance of metal-composite single bolted connections at room temperature and 250°C. The results showed that the joint strength at 250°C decreased by approximately 42% to 50% compared to room temperature, and the variation in the sequence of composite material layers had a significant effect on the connection strength at high temperatures. Cheng et al. [11] investigated the hygrothermal performance of single-layer woven T300/QY9512 laminates through experimentation and analysis. The results indicated that hygrothermal environments significantly affected the compression strength of stitched laminates, with a potential reduction of up to 50% in compression strength. Song et al. [12] conducted experimental research on the failure strength of carbon/epoxy resin single-lap riveted joints after thermal exposure, observing a 23% decrease in failure load attributed to thermal damage to the matrix. Hu et al. [13] investigated the bearing performance and failure mechanisms of interference fit joints with single-lap bolted composite materials under thermal loading through experimentation. The results showed that thermal loads play a significant role in these joints, representing a factor that cannot be overlooked as it enlarges the failure area and alters the failure mode.

Although experiments can provide intuitive information on the mechanical behavior of composite materials and their joint structures under thermal loading, conducting numerous expensive and time-consuming tests for each composite material structure is burdensome due to the diversity of composite materials and the complexity of test environments. Therefore, there is an urgent need for reliable and efficient numerical methods to predict the failure of composite material joints in structural design and analysis. At present, many numerical and analytical methods have been developed to simulate the response and failure of various composite material structures. Zhang et al. [14] proposed a progressive failure analysis model considering hygrothermal effects to predict the failure of notched composite laminates. Santiuste et al. [15] developed a finite element-based stress calculation model for anchor bolts and composite plates. The load-displacement curve, stress field, and induced damage all show significant effects of temperature and torque levels on the joints. Hu et al. [16] proposed an anisotropic continuum damage model considering temperature effects, based on continuum damage mechanics and incorporating shear nonlinear constitutive relationships described by the Romberg-Osgood equation. Wang et al. [17] developed a progressive damage model considering hygrothermal effects to analyze perforated plates made of high-strength glass fiber composite materials. They predicted the ultimate tensile and compressive strengths of the plates under room temperature, dry, and hygrothermal conditions. Shan et al. [18] employed numerical simulation methods to investigate the coupled effects of hygrothermal environment and geometric parameters on the failure of double-lap single-bolt composite joints. Gholami et al. [19] proposed a novel coupled hygm-thermo-mechanical multiscale-APFEA algorithm to accurately predict the mechanical and failure behavior of thick fiber-reinforced laminated composite materials under hygrothermal conditions.

However, there is a lack of relevant research on the failure analysis of composite-metal hybrid joints structures in thermal environments, which provides the motive of this paper. In this paper, a progressive failure analysis model considering hygrothermal effects is employed to predict the failure of composite-metal hybrid joints structures in a thermal environment. The model introduces thermal strain into the constitutive relationship and incorporates temperature corrections of material parameters into the stress analysis model, failure criteria, and material degradation laws. Tensile experiments on composite-metal hybrid joints structures are conducted under low temperature, room temperature, and elevated temperature conditions, and the experimental results are compared with numerical simulation results to validate the accuracy of the model. It is hoped that the modeling approach in this paper can provide guidance for the design and in-service application of such joints.

Footers, except for the first page, contain the page number, centered.

2. Progressive failure analysis model involving thermal effects

A progressive failure analysis model is introduced to predict the failure of composite structures under thermal conditions. The influence of thermal effects on stress analysis, failure criteria, and material degradation models for composite structures is taken into consideration by the model. The model is accompanied by a detailed flowchart, and its implementation process is elaborated upon.

2.1 Constitution equation accounting for thermal effects

Fiber-reinforced polymer composites are easily affected by thermal loadings [16]. Distinct changes in size and shape in three material principle directions of composites due to their anisotropy are caused by temperature variation. Commonly anisotropic composite material in thermal environment, in the principal material coordinate system, the strain-stress relationship is obtained by combining the thermal strains with the stress-induced strains:

$$\boldsymbol{\sigma} = \mathbf{C} \times \left(\boldsymbol{\varepsilon} - \boldsymbol{\alpha} \Delta T \right) \tag{1}$$

where σ_{ij} and ε_{ij} (i, j = 1, 2, 3) are the actual strain and stress components in the composite, respectively. $\mathbf{C}$ is the stiffness matrix. ΔT is the temperature increment. Parameters α_{ij} are the temperature expansion coefficients. For a unidirectional composite, which is transversely isotropic, the temperature do not induce shear strains. Thus the expansion coefficients satisfy the following equations: $\alpha_{12} = \alpha_{13} = \alpha_{23} = 0$. Besides, the following equations can also be obtained: $\alpha_{22} = \alpha_{33}$.

2.2 Thermal effects on the degradation of material properties

The alteration of the temperature in composites not only causes thermal strains, but also changes the mechanical behaviors of composites [20]. Dimensionless temperature T^* proposed by Tsai [21] is a basic parameter for evaluating the thermal properties of composite materials, which is defined as follows:

$$T^* = \left(T_g - T \right) \Big/ \left(T_g - T_0 \right) \tag{2}$$

where T_g and T are the glass transition temperature and current temperature, respectively; T_0 indicates the room temperature.

Based on Tsai's equation, the elastic modulus in a thermal environment can be expressed by dimensionless temperature T^* as [20]:

$$\begin{aligned} \frac{E_1^T}{E_1} &= \frac{E_2^T}{E_2} = \frac{E_3^T}{E_3} = \left(T^* \right)^a \\ \frac{G_{12}^T}{G_{12}} &= \frac{G_{13}^T}{G_{13}} = \frac{G_{23}^T}{G_{23}} = \left(T^* \right)^b \end{aligned} \tag{3}$$

where E_1, E_2, E_3, G_{12}, G_{13} and G_{23} are the basic material properties of composite materials. Their variants with superscript T represent the properties under thermal effects at temperature T. Parameters a and b are power-law indexes determined by composite materials.

Furthermore, temperature also has a significant effect on the strength of the composite. The relationship between temperature and strength can be described as follows [20]:

$$\begin{aligned} \frac{X_t^T}{X_t} &= \frac{V_f^T}{V_f} \left(T^* \right)^a \\ \frac{X_c^T}{X_c} &= \frac{Y_t^T}{Y_t} = \frac{Y_c^T}{Y_c} = \frac{Z_t^T}{Z_t} = \frac{Z_c^T}{Z_c} = \frac{V_f^T}{V_f} \left(T^* \right)^a \left(T^* \right)^b \\ \frac{S_{12}^T}{S_{12}} &= \frac{S_{13}^T}{S_{13}} = \frac{S_{23}^T}{S_{23}} = \left(T^* \right)^c \end{aligned} \tag{4}$$

where the parameters X_t, X_c, Y_t, Y_c, Z_t, Z_c, S_{12}, S_{13}, S_{23} are basic strengths of composite materials, and their variants with superscript T are strength properties under thermal effects at temperature T. V_f is the fiber volume fraction. Since temperature is generally deemed to have limited influence on the fiber volume fraction for CFRP materials, the ratio of $V_f^T = V_f$ equals to be unit.

The parameters a, b, and c are power-law indexes determined by the composite material. For CFRP materials, The parameters a = 0.04, b = 0.5, and c = 0.2.

2.3 Thermal effects on the damage initiation and propagation of the progressive failure analysis model

Due to thermal effects, the stiffness matrix of composite in Eq. (1) exhibits temperature-dependent feature:

Among the numerous failure criteria proposed for different composite structures, the Hashin-type failure criterion stands out as one of the most effective approaches for investigating failures and discerning failure modes within the framework of elastic damage mechanics [22–25]. To comprehensively characterize and distinguish composite-related failure modes, the improved Hashin failure criterion containing seven failure modes of composite laminate proposed by Shokrieh et al. [26] is as follows:

$$\mathbf{C}^T = f\left(E_1^T, E_2^T, E_3^T, G_{12}^T, G_{13}^T, G_{23}^T, v_{12}, v_{13}, v_{23}\right) \tag{5}$$

Among the numerous failure criteria proposed for different composite structures, the Hashin-type failure criterion stands out as one of the most effective approaches for investigating failures and discerning failure modes within the framework of elastic damage mechanics [22–25]. To comprehensively characterize and distinguish composite-related failure modes, the improved Hashin failure criterion containing seven failure modes of composite laminate proposed by Shokrieh et al. [26] is as follows:

$$\begin{aligned}
&\text{Fiber tension failure } (\sigma_{11} > 0): && \left(\frac{\sigma_{11}}{X_t^T}\right)^2 + \left(\frac{\sigma_{12}}{S_{12}^T}\right)^2 + \left(\frac{\sigma_{13}}{S_{13}^T}\right)^2 = 1 \\
&\text{Fiber compression failure } (\sigma_{11} < 0): && \left(\frac{\sigma_{11}}{X_c^T}\right)^2 = 1 \\
&\text{Matrix tension failure } (\sigma_{22} > 0): && \left(\frac{\sigma_{22}}{Y_t^T}\right)^2 + \left(\frac{\sigma_{12}}{S_{12}^T}\right)^2 + \left(\frac{\sigma_{23}}{S_{23}^T}\right)^2 = 1 \\
&\text{Matrix compression failure } (\sigma_{22} < 0): && \left(\frac{\sigma_{22}}{Y_c^T}\right)^2 + \left(\frac{\sigma_{12}}{S_{12}^T}\right)^2 + \left(\frac{\sigma_{23}}{S_{23}^T}\right)^2 = 1 \\
&\text{Fiber-matrix shear-out failure } (\sigma_{11} < 0): && \left(\frac{\sigma_{11}}{X_t^T}\right)^2 + \left(\frac{\sigma_{12}}{S_{12}^T}\right)^2 + \left(\frac{\sigma_{13}}{S_{13}^T}\right)^2 = 1 \\
&\text{Interlaminar tension failure } (\sigma_{33} > 0): && \left(\frac{\sigma_{33}}{Z_t^T}\right)^2 + \left(\frac{\sigma_{13}}{S_{13}^T}\right)^2 + \left(\frac{\sigma_{23}}{S_{23}^T}\right)^2 = 1 \\
&\text{Interlaminar compression failure } (\sigma_{33} < 0): && \left(\frac{\sigma_{33}}{Z_c^T}\right)^2 + \left(\frac{\sigma_{13}}{S_{13}^T}\right)^2 + \left(\frac{\sigma_{23}}{S_{23}^T}\right)^2 = 1
\end{aligned} \tag{6}$$

where σ_{ij} are the actual stresses of composite structures in thermal environment. X_t^T, X_c^T, Y_t^T, Y_c^T, Z_t^T, Z_c^T, S_{12}^T, S_{13}^T, S_{23}^T are strength parameters of composite materials. The subscript T indicates that the parameters have contained temperature effects. Thermal conditions indirectly impact the failure criteria for progressive damage by influencing the material strength.

Upon material damage, the affected material exhibits characteristics of material softening, typically marked by decreased stiffness of the material. These stiffness coefficients degrade with the reduction of elastic modulus and Poisson's ratio if damage occurs. Then the degraded stiffness coefficients, denoted by $\mathbf{C}^d$, can be written as:

$$\mathbf{C}^d = f\left(E_1^d, E_2^d, E_3^d, G_{12}^d, G_{13}^d, G_{23}^d, v_{12}^d, v_{13}^d, v_{23}^d\right) \tag{7}$$

where the superscript d represents the damaged materials. Generally, degradation factors are used to explicitly describe the reduction degree of elastic coefficients. The elastic coefficients can be expressed by a multiplying of the degradation factor and its initial value.

Zhang[27] improved the Tserpes drop degradation model based on micromechanics to characterize the degradation of material element stiffness under the above seven failure modes. This material degradation model is used in this study. Table 1 list the relationship among the failure modes, elastic coefficients, and degradation factors. The degradation factor for each row corresponds to the failure mode, and the degradation factor for each column relates to the corresponding elastic coefficient. d_{ft} represents the degradation factor for fiber tension failure, d_{fc} for fiber compression failure, d_{mt} for Matrix tension failure, d_{mc} for Matrix compression failure, d_{fm1} and d_{fm2} for fiber–matrix shear-out failure, d_{dt} for Interlaminar tension failure, d_{dc} for Interlaminar compression failure. The degradation factor is expressed as:

$$
\begin{aligned}
&d_{ft}=\frac{V_m E_m^T}{E_1^T}, d_{fc}\approx\frac{E_2^T}{E_1^T}\\
&d_{mt}=d_{dt}=0, d_{mc}=d_{dc}\approx 0\\
&d_{fm1}=\left(\frac{1-\sqrt{V_f}}{1-\sqrt{V_f}+V_f}\right)\frac{G_m^T}{G_{12}^T}\\
&d_{fm2}=\left(\frac{1-\sqrt{V_f}}{1-\sqrt{V_f}+V_f}\right)\frac{G_m^T}{G_{23}^T}
\end{aligned}
\tag{8}
$$

where E_m and G_m are the elastic modulus of the composite matrix, the subscript indicates that the parameters have contained temperature effects. V_m is the matrix volume fraction.

Table 1 Material degradation model for the Hashin-type failure criterion

Failure mode	Degradation factors								
	E_1^T	E_2^T	E_3^T	G_{12}^T	G_{13}^T	G_{23}^T	v_{12}	v_{13}	v_{23}
Fiber tension	d_{ft}	1	1	1	1	1	1	1	1
Fiber compression	d_{fc}	1	1	1	1	1	1	1	1
Matrix tension	1	d_{mt}	1	d_{mt}	1	d_{mt}	d_{mt}	1	d_{mt}
Matrix compression	1	d_{mc}	1	d_{mc}	1	d_{mc}	d_{mc}	1	d_{mc}
Fiber–matrix shear-out	1	1	1	d_{fm1}	d_{fm1}	d_{fm2}	d_{fm1}	d_{fm1}	d_{fm2}
Interlaminar tension	1	1	d_{dt}	1	d_{dt}	d_{dt}	1	d_{dt}	d_{dt}
Interlaminar compression	1	1	d_{dc}	1	d_{dc}	d_{dc}	1	d_{dc}	d_{dc}

The thermal environment has little effect on the mechanical properties of metal materials, but the thermal expansion coefficient of metal materials is much higher than that of composite materials, resulting in the heating stress inside the connected structure when the temperature changes, so it should be taken into account in modeling. The actual loading process will be accompanied by the plastic deformation of metal materials. In ABAQUS®, the plasticity of materials is set by a series of corresponding data of real stress and plastic strain.

Based on the above continuum failure analysis model considering thermal effects, the user defined subroutine UMAT contains the above failure criterion and material degradation under thermal effects is embedded into the general finite element analysis program ABAQUS®. The flow chart of the model is shown in Fig. 1, thus a nonlinear continuum failure analysis of the composite material, metal material and its joint structures can be implemented under thermal conditions.

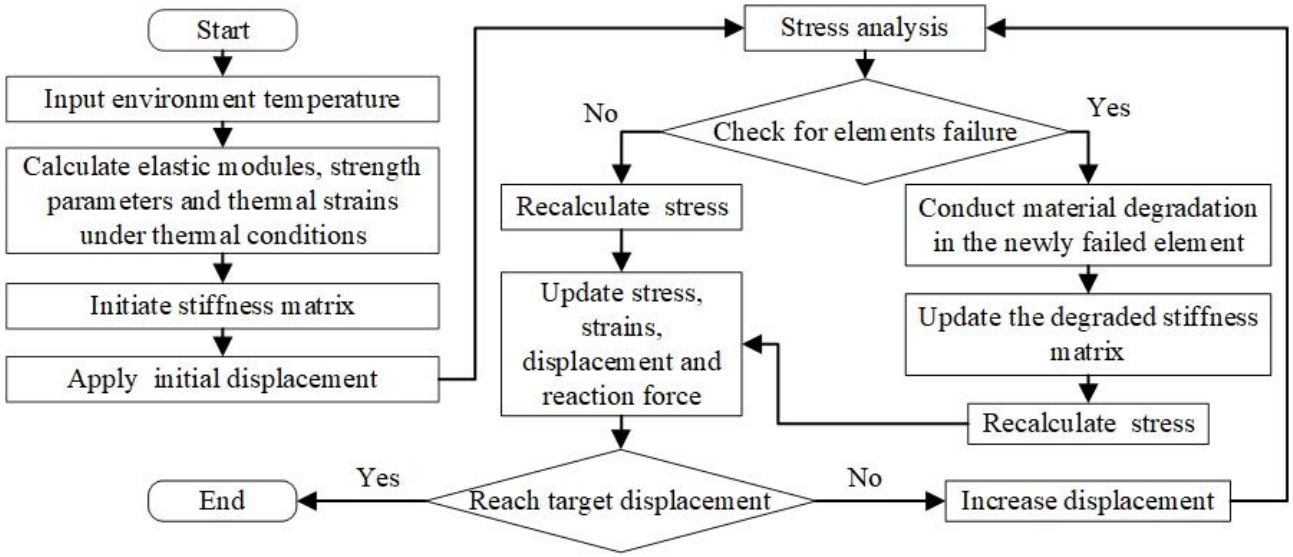

Figure 1 – Flowchart of continuum damage model under thermal effects.

3. Specimens and experimental procedures

3.1 Specimens

The specimens were CFRP composite and aluminum alloy triple bolt double-lap joint forms, in which the composite laminate was made of T800 grade carbon fibers and epoxy resin, and the laminate was laid in the sequence of $[45/0/-45/90/0/0/45/0/-45/0]_{2s}$, with nominal thickness t_C=5.6mm. The unidirectional strip is an orthotropic material with a single layer thickness of 0.14mm. The material properties are shown in Table 2. The metal plate material is 7075/T7451 aluminum alloy, the thickness is t_{Alum}=5.6mm, the elastic modulus is 74.5 GPa, the Poisson ratio is 0.3, and the thermal expansion coefficient is 2.25×10^{-5}. The bolt is made of titanium alloy, the bolt diameter D is 8mm, and the tightening torque T=14N/m. The bolt is made of 6Al-4V titanium alloy material with an elastic modulus of 112GPa, Poisson's ratio of 0.34, yield strength of 909MPa, and coefficient of thermal expansion of 9.1×10^{-6}. The size of the specimen is shown in Fig. 2, and the length of the two lap plates is 272mm. Connector row distance aperture ratio p/D = 4.5, side distance aperture ratio Sw/D=3, end distance aperture ratio e/D=3.

Table 2 Mechanical properties of composite lamina.[28]

Elastic properties	E_1 /GPa	E_2 /GPa	E_3 /GPa	G_{12} /GPa	G_{13} /GPa	G_{23} /Gpa	ν_{12}	ν_{13}	ν_{23}
	157.6	8.295	8.295	4.37	4.37	3.26	0.33	0.33	0.33
Strength properties	X_t /MPa	X_c /MPa	Y_t /Mpa	Y_c /MPa	Z_t /MPa	Z_c /MPa	S_{12} /MPa	S_{13} /MPa	S_{23} /MPa
	2681	1545	76.58	214.8	76.58	214.8	154	154	154

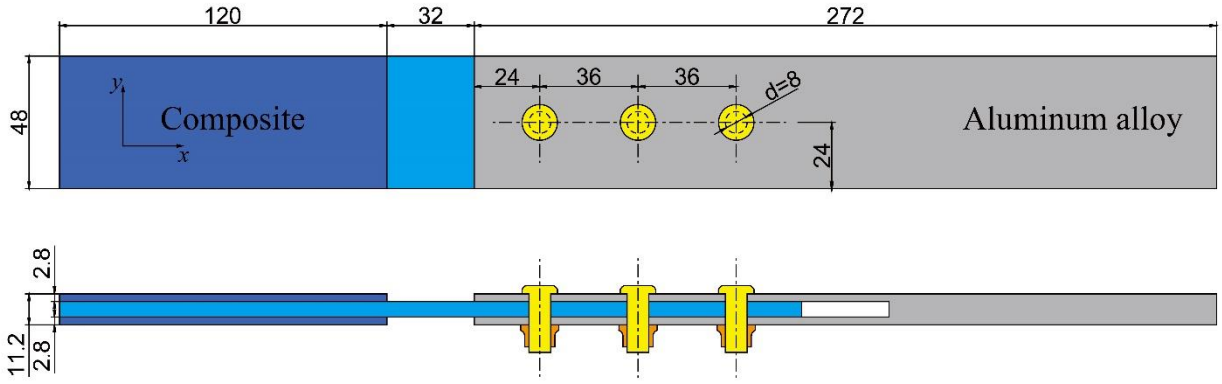

Figure 2 – Geometric information and dimensions of specimen.

3.2 Static strength tests

According to the test standard ASTM D5961/D5961M-17, the tensile test was carried out on the electronic universal test machine. The test is stopped when the load is applied at a constant beam displacement rate of 2mm/s until the test piece is completely destroyed or the load curve suddenly drops. During the experiment, the ambient temperature is controlled by the high and low temperature environment test chamber, and the high and low temperature environment is realized by the high-temperature alloy heating tube and the refrigeration compressor respectively. The strain data and load-displacement data were continuously collected by digital data acquisition system. The peak value of load-displacement curve was taken as the ultimate failure load, and the failure mode of the specimen was recorded by photographs. The experimental setup is shown in Fig. 3.

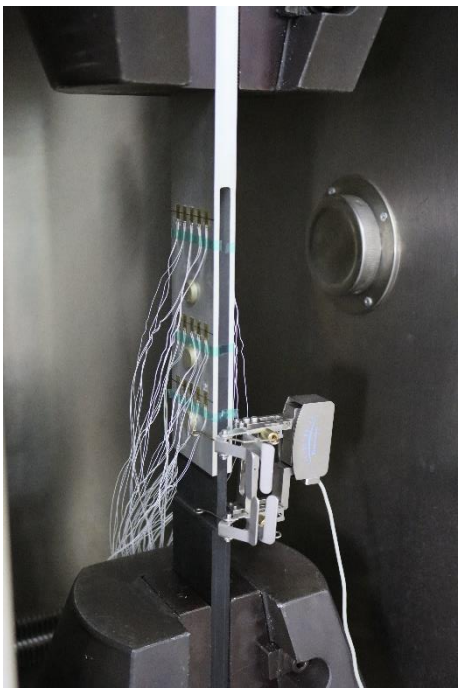

Figure 3 – Tensile test of composite-metal hybrid Joints.

4. Finite element models and experimental validation

4.1 Models of composite-metal joints structure concerning thermal effects

The 3D finite element model of the composite-metal triple bolts double shear joint structure in thermal conditions was conducted by ABAQUS® for accurate stress analysis. The structural finite element model is shown in Fig. 4, with the entire mesh being comprised of linear fully integrated C3D8 eight-node solid elements, with three displacement degrees of freedom per node. For the composite laminate, one element is established for every four plies in the thickness direction, while five elements are established for the metal plate in the thickness direction. Around the connection plate hole, 84 seeds are uniformly set, ensuring consistent mesh distribution on the contact surfaces. The friction coefficient between the bolt and the connection plate is 0.1, and the friction coefficient between connection plates is 0.2.

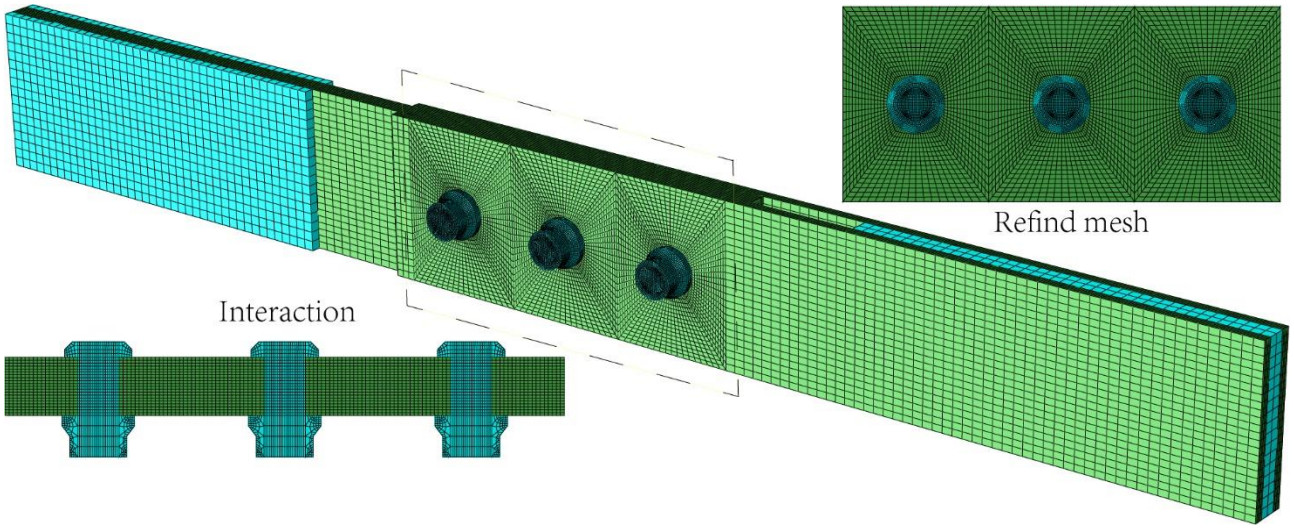

Figure 4 – Finite element model of composite-metal hybrid joints.

The thermal effects were introduced into the finite element analysis from two aspects: the stress-strain relationship of the composite material accounted for the temperature influence; the material stiffness matrix, as shown in Eq. (5), includes temperature influence in the strength parameters. Additionally, the material degradation model in Eq. (6) and Table 1 establishes a progressive failure analysis model. The degradation factors in Table 1 are calculated using Eq. (8) and the basic material parameters in Table 2, as shown below:

d_{ft}=0.00833, d_{fc}=0.0297, d_{fm1}=0.0683, d_{fm2}=0.0915.

The d_{mt}, d_{mc}, d_{dt} and d_{dc} equal to zero, which means that the corresponding elastic coefficients will be degraded to zero. To avoid numerical convergence problems, they were set to be 10^{-6}.

Based on the aforementioned numerical model, a progressive failure analysis of composite-metal joints structures under thermal conditions has been implemented.

4.2 The Influence of temperature on the ultimate load

In the experimental process, the maximum load is taken as the structural failure load, and five tests are conducted under the same temperature environment. Table 3 lists the average failure load, variance, coefficient of variation, predicted failure load, and error data for comparing the experimental and simulation results. It can be seen that the coefficient of variation does not exceed 2.16%, indicating good consistency in the experimental results. The maximum dispersion of data at -75°C low temperature environment is 2.16%. The maximum relative error of predicted failure load for all specimens is only 5.2%, indicating good agreement between numerical calculation results and corresponding experimental average failure loads. Therefore, the progressive failure analysis model it follows can accurately predict the failure of composite material-metal bolt connection structures under thermal effects in the current investigation.

Table 3 Comparison between test value and simulation value.

Temperature/℃	Failure load/kN	Standard deviations	Dispersion coefficient/%	Numerical result/kN	Error/%
-75	117.58	6.45	2.16%	123.69	5.2
25	113.91	1.13	0.93%	116.41	2.2
120	105.61	0.93	0.91%	109.52	3.7

The load–displacement curves obtained at -75℃, 25℃ and 120℃ are shown in Fig. 5. The limit load of the specimen at -75℃ is 117.5kN, which is slightly higher than the limit load at 25℃ of 113.9kN. Low temperature causes the cold hardening of the resin matrix, enhances the stiffness of the material, and enhances the bearing capacity of the structure to a certain extent. However, low temperature also makes the material brittle, and small damage is easy to expand rapidly, resulting in premature failure of the structure. At 120℃, the ultimate load of the specimen is 105.8kN, which is 7.11% lower than that at room temperature. This is due to the joint action of resin thermal softening, residual stress relaxation and thermal expansion of the joint components under elevated temperature environment, and the b

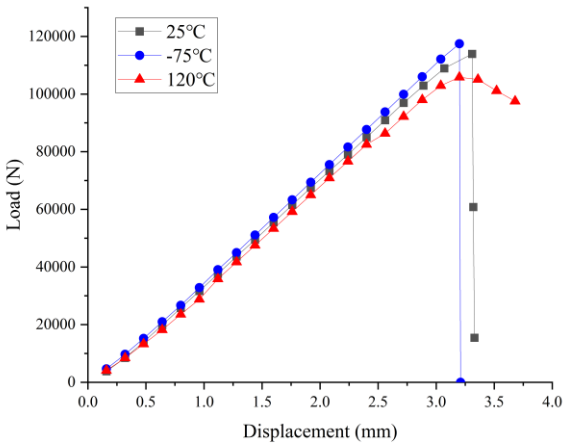

Figure 5 – Tensile response of composites under thermal effects.

Through the progressive failure analysis, the failure behavior of each group of specimens were predicted. The tensile sample at 120℃ are taken as an example to expatiate the numerical results and their comparisons with experimental outcomes. The predicted tensile load-displacement curve combined with the experimental data is shown in Fig. 6. Prior to the sudden drop in load, the load-displacement curves of the specimens exhibit almost linear behavior. The predicted initial stiffness aligns well with the experimental results, confirming the accuracy of the finite element model used. As the applied load increases, the slope of the numerical curve gradually decreases until it reaches zero, indicating the peak load. Subsequently, the slope further decreases and the load drops. Notably,

the predicted peak loads in the graph fall within the range of test failure loads, providing supporting evidence for the effectiveness of the progressive failure analysis model.

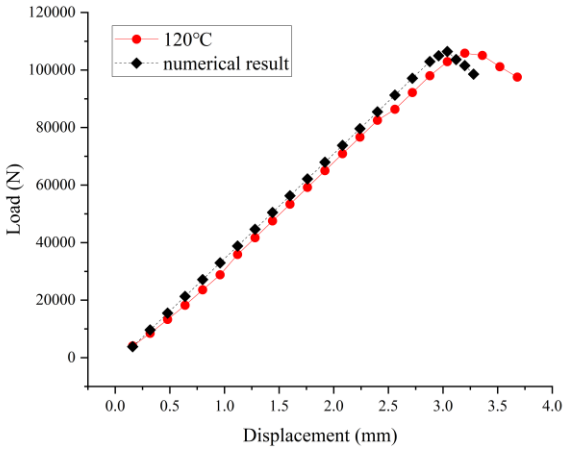

Figure 6 – Comparison of load-displacement curve of tensile test at 120℃ and simulation results.

4.3 The Influence of temperature on the failure modes and failure process of hole-edge damage

Structural failure caused by the tensile fracture of the composite overlap plate near the clamping side hole at -75℃ in the composite-metal hybrid joints structure is shown in Fig. 7. In the low-temperature environment, tensile fracture occurs along the edge of hole 1, while compression occurs at the edges of holes 2 and 3 without significant expansion. This is because the low temperature increases the structural stiffness. However, when the load reaches the limit value, the damage at the hole edge will rapidly propagate, leading to brittle fracture of the structure. This is because the low temperature increases the structural stiffness. However, when the load reaches the limit value, the damage at the hole edge will rapidly propagate, leading to brittle fracture of the structure. At temperatures of 25°C and 120℃, the compression failure of the hole edge in the composite overlap plate occurs. At 120℃, the degree of compression deformation at the hole edge is more severe than at 25°C due to the softening of the resin matrix and the material's increased plasticity at elevated temperatures, making the structure more prone to hole edge damage under loading. In aircraft structural design, to avoid catastrophic failure of the structure, it is usually desired that the failure mode of the structure be hole edge compression failure.

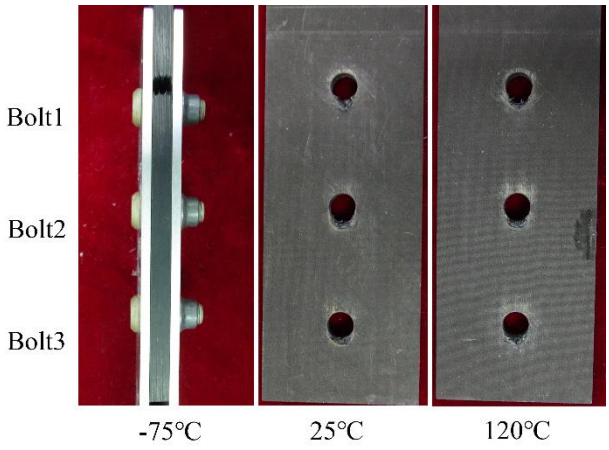

Figure 7 – Macroscopic failure mode of composite-metal hybrid joints.

Due to the fact that the load-bearing failure of the composite-metal hybrid joints structure is mainly caused by damage to the composite material hole edges, the cross-section of the composite material hole edges was selected for analysis. To compare the influence of temperature on the damage pattern of the hole edges in the composite material structure, Fig. 8 presents the evolution process of fiber damage at the hole edges of the composite material in three different temperature environments. At -75℃ and 120℃, the distribution patterns of damage at hole edges are significantly different. At -75℃, the thermal expansion coefficients of the metal and composite materials are

different, leading to shrinkage of the metal and the generation of thermal stress at the hole edges. At this time, the thermal stress on Hole 1 is in the same direction as the compressive load, so the damage at the hole edge first appears at Hole 1. As the load increases, the damage continues to expand, and when the ultimate load is reached, the damage at the hole edge of Hole 1 rapidly expands, causing the composite material plate to fail in tension. At 120℃, the expansion of the metal is significant. At this time, the thermal stress on Hole 3 is in the same direction as the compressive load, so the damage at the hole edge first appears at the hole edge of Hole 3. Additionally, due to the influence of elevated temperature, the damaged regions is larger at 120℃.

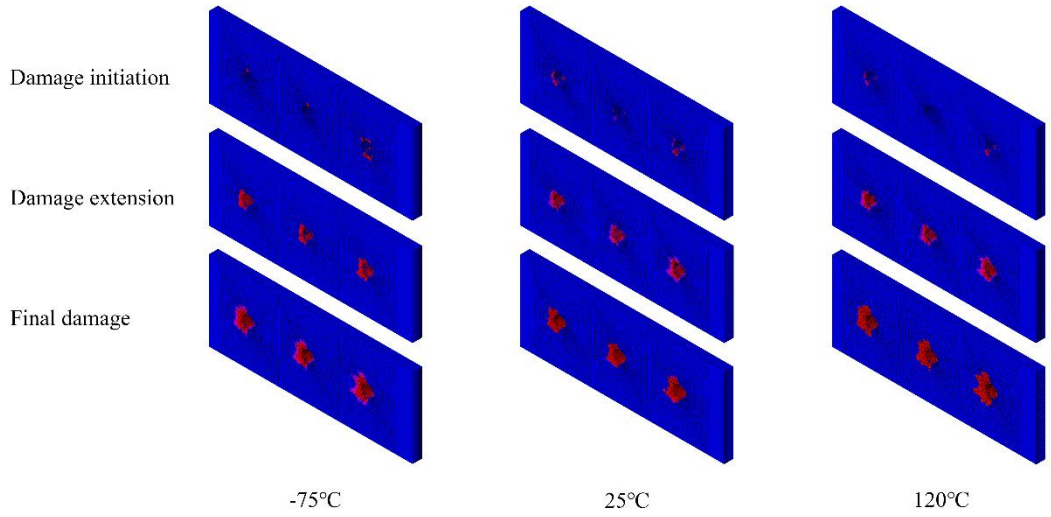

Figure 8 – The evolution of fiber damage at hole edges in composite materials under different temperatures.

In the experiment, the ratio of the load by each bolt is calculated by the ratio of the average strain between two holes to the total strain of the overlap plate, as shown in Fig. 9. At the beginning of loading, due to friction between the overlap plates and the presence of gaps between the bolts, the proportion of bolt loads continues to change. When the load reaches 0.4 Fmax, the proportions of loads on Bolts 1, Bolts 2, and Bolts 3 are 4:2.5:3.5, and they remain stable. As the load increases, damage occurs at the hole edge of Hole 1, transferring the load from Bolt 1 to Bolt 2. When the ultimate load is reached, all holes experience compressive damage leading to structural failure. At 25℃, damage initially appears at the hole edges of the two holes bearing the larger load, and as the load transfers, eventually all three holes experience compressive failure.

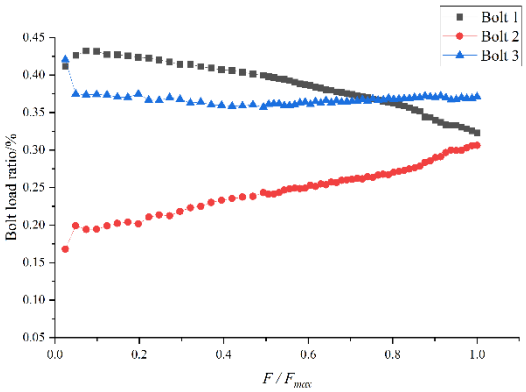

Figure 9 – Bolt-load distribution ratio at 25℃

5. Conclusions

For the Composite-Metal Hybrid Joints structure, static tests were conducted under three different environmental conditions: low temperature, room temperature, and elevated temperature. In order to predict the failure of the Composite-Metal Hybrid Joints structure under thermal influence, a finite element model of the Composite-Metal Hybrid Joints structure was established for failure analysis of composite material structures under thermal influence. The main conclusions drawn are as follows:

(1) The numerical model can effectively describe stress evolution, component deformation, and damaged regions. The numerical results of the calculations align closely with the experimental findings, confirming the model's efficacy in precisely forecasting the failure of composite laminate panels under thermal effects.

(2) Elevated temperatures primarily contribute to the expansion of damaged areas in composite materials, as the heat softens the resin matrix, leading to a notable decrease in compressive properties. Conversely, low temperatures induce cold hardening of the resin matrix, improving material stiffness and enhancing the structural load-bearing capacity to some extent. Nevertheless, lower temperatures also induce material brittleness, facilitating rapid damage propagation and ultimately leading to premature structural failure.

(3) The composite-metal hybrid joints structure exhibits different locations of damage initiation at various temperatures. At low temperatures, damage first occurs at the edge of hole 1. However, at elevated temperatures, damage initiates at the edge of hole 3. This is attributed to the thermal expansion coefficient difference between the composite and metal materials, leading to thermal stress in the structure. When thermal stress combines with mechanical loads, it causes uneven distribution of loads on the bolts, resulting in a change in the location of damage initiation.

(4) The composite-metal hybrid joints structure experiences hole compression failure as the predominant failure mode at room temperature and elevated temperatures, which is desired during structural design. However, at low temperatures, thermal stress generation and material cold hardening result in tensile fracture of the overlap plate. Therefore, thermal effects must be considered in structural design and analysis.

6. Contact Author Email Address

mailto: rui_h@126.com

7. Copyright Statement

References

[1] Zhao Z, Dang H, Zhang C, Yun G J, Li Y. A multi-scale modeling framework for impact damage simulation of triaxially braided composites. *Compos Part Appl Sci Manuf*, vol. 110, pp. 113–125, 2018.

[2] Yang G, Park M, Park S J. Recent progresses of fabrication and characterization of fibers-reinforced composites: A review, *Compos Commun*, vol. 14, pp. 34–42, 2019.

[3] Thoppul S. D, Finegan J, Gibson R F. Mechanics of mechanically fastened joints in polymer–matrix composite structures – A review, *Compos Sci Technol*. vol. 69, no. 3–4, pp. 301–329, 2009.

[4] Cao Z and Zuo Y. Electromagnetic riveting technique and its applications. *Chin J Aeronaut*, vol. 33, no. 1, pp. 5–15, 2020.

[5] Abdus S, Cheng X, Huang W, Ahmed A, Hu R. Bearing failure and influence factors analysis of metal-to-composite bolted joints at high temperature. *J Braz Soc Mech Sci Eng*, vol. 41, no. 7, p. 298, 2019.

[6] Mariam M et al. Hydrothermal ageing effect on the mechanical behaviour and fatigue response of aluminium alloy/glass/epoxy hybrid composite single lap joints. *Compos Struct*, vol. 219, pp. 69–82, 2019.

[7] Turvey G J, Sana A. Pultruded GFRP double-lap single-bolt tension joints – Temperature effects on mean and characteristic failure stresses and knock-down factors. *Compos Struct*, vol. 153, pp. 624–631, 2016.

[8] Sánchez-Sáez S, Gómez-del Río T, Barbero E, Zaera R, and Navarro C, Static behavior of CFRPs at low temperatures. *Compos. Part B Eng*, vol. 33, no. 5, pp. 383–390, 2002.

[9] Vieille B, Aucher J, Taleb L, Influence of temperature on the behavior of carbon fiber fabrics reinforced PPS laminates. *Mater Sci Eng A*, vol. 517, no. 1–2, pp. 51–60, 2009.

[10] Vieille B, Aucher J, Taleb L. Comparative study on the behavior of woven-ply reinforced thermoplastic or thermosetting laminates under severe environmental conditions. *Mater Des*, vol. 35, pp. 707–719, 2012

[11] Cheng X Q, Baig Y, Li Z H. Effects of hygrothermal environmental conditions on compressive strength of CFRP stitched laminates. *J Reinf Plast Compos.* vol. 30, no. 2, pp. 110–122, 2011.

[12] Song M H et al. An experimental study on the failure of carbon/epoxy single lap riveted joints after thermal exposure. *Compos Struct*, vol. 86, no. 1–3, pp. 125–134, 2008.

[13] Hu J, Mi S, Yang Z, Wang C, Yang Y, and Tian W. An experimental investigation on bearing behavior and failure mechanism of bolted composite interference-fit joints under thermal effects. *Eng Fail Anal*, vol. 131, p. 105830, 2022.

[14] Zhang J, Qi D, Zhou L, Zhao L, Hu N. A progressive failure analysis model for composite structures in hygrothermal environments. *Compos Struct*, vol. 133, pp. 331–342, 2015.

[15] Santiuste C, Barbero E, Henar Miguélez M. Computational analysis of temperature effect in composite bolted joints for aeronautical applications. *J Reinf Plast Compos*, vol. 30, no. 1, pp. 3–11, 2011

[16] Hu J, Zhang K, Cheng H, Zou P. Modeling on mechanical behavior and damage evolution of single-lap bolted composite interference-fit joints under thermal effects. *Chin J Aeronaut.* vol. 34, no. 8, pp. 230–244, 2021

[17] Wang X, Jia P, Wang B. Progressive failure model of high strength glass fiber composite structure in hygrothermal environment. *Compos Struct*, vol. 280, p. 114932, 2022.

[18] Shan M, Zhang R, Gong Y, Zhao L. Revealing the coupled effects of hygrothermal environment and geometrical parameters on the failure of double-lap, single-bolt composite joints. *J Mater Res Technol*, vol. 24, pp. 8282–8295, 2023.

[19] Gholami M, Afrasiab H, Baghestani A M, and Fathi A. Mechanical and failure analysis of thick composites under hygrothermal conditions by a novel coupled hygro-thermo-mechanical multiscale algorithm. *Compos Sci Technol*, vol. 230, p. 109773, 2022.

[20] Benkhedda A, Tounsi A, Adda Bedia E A, Effect of temperature and humidity on transient hygrothermal stresses during moisture desorption in laminated composite plates. *Compos Struct*, vol. 82, no. 4, pp. 629–635, 2008.

[21] Tsai S, *Composite design*, 4th edition, Dayton: Think Composites, 1988

[22] Camanho P P, Matthews F L. A Progressive Damage Model for Mechanically Fastened Joints in Composite Laminates. *J Compos Mater*, vol. 33, no. 24, pp. 2248–2280, 1999.

[23] Cheng X Q, Yang M M, Zhang J, Zhang Q, Zhang J K. Thermal behavior and tensile properties of composite joints

with bonded embedded metal plate under thermal circumstance. *Compos Part B Eng*, vol. 99, pp. 340–347, 2016.

[24]Chang F K, Chang K Y. Post-Failure Analysis of Bolted Composite Joints in Tension or Shear-Out Mode Failure. *J Compos Mater*, vol. 21, no. 9, pp. 809–833, 1987.

[25]Chang F K, Chang K Y. A Progressive Damage Model for Laminated Composites Containing Stress Concentrations, *J Compos Mater*, vol. 21, no. 9, pp. 834–855, 1987

[26]Poon C, Lessard L, Shokrieh M. Three dimensional progressive failure analysis of pin/bolt loaded composite laminates. *The 83rd meeting of the AGARD SMP on bolted joints in polymeric composites*, Italy, 1996.

[27]Zhang J, Zhou L, Chen Y, Zhao L, Fei B. A micromechanics-based degradation model for composite progressive damage analysis. *J Compos Mater*, vol. 50, no. 16, pp. 2271–2287, 2016.

[28]Zhang D, Zhou J, Wang J, Zhang W, Guan Z. A comparative study on failure mechanisms of open-hole and filled-hole composite laminates: Experiment and numerical simulation. *Thin-Walled Struct*, vol. 198, p. 111730, 2024.